ARTICLE
Journal of Cellular Biochemistry 113:3762–3772 (2012)

Journal of Cellular Biochemistry

Quantitative Proteome Analysis of Ovarian Cancer Tissues Using a iTRAQ Approach

Li-Na Wang,[1,2] Shi-Wen Tong,[1] Huai-Dong Hu,[1] Feng Ye,[1] Sang-Lin Li,[1] Hong Ren,[1] Da-Zhi Zhang,[1] Rong Xiang,[1,2*] and Yi-Xuan Yang[1**]

[1]*Key Laboratory of Molecular Biology for Infectious Diseases of Ministry of Education of China, The Second Affiliated Hospital, Chongqing Medical University, Chongqing 400016, China*

[2]*Department of Immunology, Nankai University School of Medicine, Tianjin 300071, China*

ABSTRACT

Quantitative proteomics can be used as a screening tool for identification of differentially expressed proteins as potential biomarkers for cancers. Here, we comparatively analyzed the proteome profiles of ovarian cancer tissues and normal ovarian epithelial tissues. Using the high-throughput proteomic technology of isobaric tags for relative and absolute quantitation (iTRAQ)-coupled with two-dimensional-liquid chromatography-tandem mass spectrometry, 1,259 unique proteins were identified. Of those, 205 were potentially differentially expressed between ovarian cancer and normal ovarian tissues. Several of the potentially differentially expressed proteins were validated by Western blotting and real-time quantitative RT-PCR analyses. Furthermore, up-regulation of KRT8, PPA1, IDH2, and S100A11 were validated in ovarian tissue microarrays by immunohistochemistry. Silencing of S100A11 expression suppressed the migration and invasion properties of ovarian cancer cells in vitro. Our study represents the successful application of iTRAQ technology to an investigation of ovarian cancer. Many of the potentially differentially expressed proteins identified had not been linked to ovarian cancer before, and provide valuable novel insights into the underlying mechanisms of carcinogenesis in human ovarian cancer. J. Cell. Biochem. 113: 3762–3772, 2012.

KEY WORDS: OVARIAN CANCER; PROTEOMICS; iTRAQ; MASS SPECTROMETRY

Ovarian cancer is the leading cause of death among the gynecological cancers [Banerjee and Gore, 2009]. The major reason for poor outcome is that most patients had advanced stage of ovarian cancer at the time of diagnosis when cancer has metastasized and surgery is not a viable option. Early detection of ovarian cancer offers the best chance for cure. Unfortunately, tumor biomarkers, such as CEA and CA-125, that are currently utilized for the detection of ovarian cancer in clinical practice lack the sensitivity and specificity needed to detect potentially curable lesions, and therefore not suitable for population screening [Yurkovetsky et al., 2010]. Consequently, discovery of the ovarian cancer biomarkers remains a worthy task.

Over the past decades, many global gene and protein expression studies have been conducted in attempts to identify novel ovarian cancer markers. For example, a cDNA microarray analysis of secretory proteins that differ between ovarian cancer cells and normal human ovarian surface epithelial cells by Mok et al. [2001] revealed prostasin to be a potential biomarker of human ovarian cancer [Kim et al., 2005]. In another study, by an iterative searching algorithm Petricoin et al. [2002] analyzed serum from 50 unaffected women and 50 patients with ovarian cancer using SELDI-TOF-MS. The algorithm identified a cluster pattern, which completely segregated cancer from non-cancer in the training set. Although the differential profiling of ovarian cancers has yielded numerous insights into the biology of ovarian cancers and novel therapeutic and imaging targets, the results in terms of biomarker discovery have been less striking. There are two potential causes for the small fraction of differentially expressed transcripts or proteins in ovarian

Li-Na Wang, Shi-Wen Tong, and Huai-Dong Hu contributed equally to this work.

Additional supporting information may be found in the online version of this article.

*Correspondence to: Prof. Rong Xiang, Department of Immunology, Nankai University School of Medicine, Tianjin 300071, China. E-mail: rxiang@nankai.edu.cn

**Correspondence to: Dr. Yi-Xuan Yang, Key Laboratory of Molecular Biology for Infectious Diseases of Ministry of Education of China, the Second Affiliated Hospital, Chongqing Medical University, Chongqing, China
E-mail: yixuan.yang@hotmail.com

Manuscript Received: 20 February 2012; Manuscript Accepted: 3 July 2012

Accepted manuscript online in Wiley Online Library (wileyonlinelibrary.com): 13 July 2012

DOI 10.1002/jcb.24250 • © 2012 Wiley Periodicals, Inc.

cancer that translate into effective biomarkers. First, there may be significant dissociation between overexpressed transcripts and overexpressed proteins [Wulfkuhle et al., 2002]. Second, most proteomics studies in ovarian cancer have focused on blood samples, and most of the found biomarkers in serum or plasma are acute phase proteins, which are not linked to a specific cancer or disease [Cortesi et al., 2011].

In ovarian cancer studies using tumor tissues are sparse. It would be interesting to investigate proteome of the ovarian cancer tissue in an attempt to overcome acute phase reactants and to facilitate the discovery of real tumor-specific biomarkers. Over the past 5 years there has been an increasing interest in applying isotope-based quantitative proteomics for research of diverse fields—ranging from biomarker discovery to post-translational modifications. These emerging technologies include ICAT, isobaric tags for relative and absolute quantitation (iTRAQ), ^{18}O, and stable isotope labeling with amino acids in cell culture (SILAC) [Gygi et al., 1999; Mirgorodskaya et al., 2000; Ross et al., 2004]. Among these, the iTRAQ method is a powerful tool in which up to eight samples can be analyzed in one experiment. In the current study, we employed iTRAQ to identify alterations in the proteome between ovarian cancer and normal ovarian epithelia tissues that might be associated with the development and progression of ovarian cancer. The findings from our study may greatly expand the number of our candidate biomarkers of ovarian cancer.

MATERIALS AND METHODS

TISSUE SAMPLES AND CELL LINES

The study was performed after approval by the Institutional Review Boards for Human Subject Review at Nankai University. From July 2009 to July 2010, ovarian cancer tissues (n = 8, including three serous adenocarcinomas, three mucinous adenocarcinomas, and two endometrioid carcinomas) were collected from patients with primary epithelial ovarian cancer. Normal ovarian epithelial tissues (n = 8) during the same period of time were also collected from patients at the Tianjin Central Hospital for Obstetrics and Gynecology.

The human ovarian cancer cell lines, ES-2 and SKOV-3 were originated from the American Type Culture Collection. These cells were cultured in RPMI1640 medium containing 10% fetal calf serum.

REAGENTS

The iTRAQ kits were purchased from Applied Biosystems (Foster City, CA). Sequence grade modified trypsin was purchased from Promega (Madison, WI). PVDF membrane, goat anti-mouse, goat anti-rabbit, or rabbit anti-goat IgG-conjugated with horseradish peroxidase, and the enhanced chemiluminescence (ECL) system were purchased from Amersham Biosciences(Uppsala, Sweden). Monoclonal or polyclonal antibodies against KRT8, PPA1, IDH2, S100A11, and actin were from Abcam (Cambridge, MA).

PROTEIN SAMPLE PREPARATION AND iTRAQ LABELING

Total protein extracts were prepared by the Sample Grinding Kit from Amersham in lysis buffer (7 M urea, 1 mg/ml DNase I, 1 mM Na_3VO_4, and 1 mM PMSF) and prior subjected to centrifugal at 15,000*g* for 30 min at 4°C. The supernatant was collected and the concentration of the total proteins was determined using 2D Quantification kit (Amersham Biosciences). Before iTRAQ labeling, equal amounts of protein from eight patients with primary epithelial ovarian cancer or eight non-cancer patients were pooled to form two final samples. From each sample, 100 μg of proteins were acetone precipitated overnight at −20°C and dissolved in the lysis buffer, denatured, and then cysteines were blocked as described in the iTRAQ protocol (Applied Biosystems, Framingham, MA). Each sample was digested with 20 μl of 0.1 μg/μl trypsin (Promega) solution at 37°C overnight and then labeled with the iTRAQ tags as follows: (i) normal ovarian epithelial tissues—113 and 115 tags, (ii) ovarian cancer tissues—114 and 116 tags. The labeled samples were pooled prior to further analysis.

STRONG CATION EXCHANGE CHROMATOGRAPHY

To reduce the sample's complexity during LC-MS/MS analysis, the pooled samples were diluted 10-fold with SCX buffer A (10 mM KH_2PO_4 in 25% acetonitrile at pH 3.0) and subjected to a 2.1 mm × 200 mm polysulfoethyl A SCX column (Poly LC, Columbia, MD). The column was eluted with a gradient of 0–25% SCX buffer B (10 mM KH_2PO_4 at pH3.0 in 25% acetonitrile containing 350 mM KCl) over 30 min, followed by a gradient of 25–100% SCX buffer B over 40 min. The fractions were collected at 1-min intervals. These SCX fractions were lyophilized in a vacuum concentrator, and subjected to C-18 clean-up using a C18 Discovery® DSC-18 SPE column (100 mg capacity, Supelco; Sigma–Aldrich, MO). The cleaned fractions were then lyophilized again and stored at −20°C prior to mass spectrometric analysis.

MASS SPECTROMETRIC ANALYSIS

Mass spectrometric analysis was performed using a nano-LC-coupled online to a QStar Elite mass spectrometer (Applied Biosystems). Peptides were loaded on a 75 μm × 15 cm, 3 μm fused silica C18 capillary column, followed by a mobile phase elution: buffer A (0.1% formic acid in 2% acetonitrile) and buffer B (0.1% formic acid in 98% acetonitrile). The peptides were eluted from 2% buffer B to 100% buffer B over 60 min at a flow rate 300 nl/min. The LC eluent was directed to ESI source for Q-TOF-MS analysis. The mass spectrometer was set to perform information-dependent acquisition (IDA) in the positive ion mode, with a selected mass range of 300–2,000 m/z. Peptides with +2 to +4 charge states were selected for tandem mass spectrometry, and the time of summation of MS/MS events was set to 3 s. The two most abundantly charged peptides above a 10 count threshold were selected for MS/MS and dynamically excluded for 60 s with ±50 mmu mass tolerance.

Peptide identification and quantification were performed using ProteinPilot software packages (Applied Biosystems). Each MS/MS spectrum was searched against the IPI human protein database v3.49 and protein identification was accepted based on ProteinPilot confidence scores. Relative quantification of proteins, in the case of iTRAQ, is performed on the MS/MS scans and is the ratio of the areas under the peaks at 113, 114, 115, and 116 Da, which were the masses of the tags that correspond to the iTRAQ reagents. Error factor (EF) and *P*-value are calculated using ProteinPilot software which gave

an indication of the deviation and significance in the protein quantification.

REAL-TIME QUANTITATIVE RT-PCR ANALYSIS

Total RNA was extracted using Trizol (Gibco BRL, MD) following the manufacturer's instructions. Two micrograms of total RNA was reverse-transcribed into first-strand cDNA using A3500 Reverse Transcription System (Promega). Quantitative RT-PCR was performed on the ABI 7900HT system using the Taq-Man Gene Expression Assay Kit and gene-specific primers for 18S (Hs99999901_s1), LAP3 (Hs01099401_g1), IDH2 (Hs00158033_m1), MX1 (Hs00895608_m1), AGR2 (Hs00180702_m1), THBS1 (Hs00962908_m1), KRT8 (Hs01595539_g1), KRT7 (Hs00559840_m1), PSAT1 (Hs00795278_mH), PPA1 (Hs01067932_g1), EPPK1 (Hs01104050_s1), S100A11 (Hs00271612_m1), MFAP4 (Hs00412974_m1), AOC3 (Hs00186647_m1), and RBP1 (Hs01011512_g1). The relative quantification of gene expression was analyzed by the $2^{-\Delta\Delta CT}$ method [Livak and Schmittgen, 2001]. Real-time quantitative RT-PCR analysis was repeated at least three times.

WESTERN BLOTTING ANALYSIS

The tissues/cells were lysed at 4°C for 30 min in a lysis buffer (50 mM Tris, pH 7.4, 100 mM $NaCl_2$, 1 mM $MgCl_2$, 2.5 mM Na_3VO_4, 1 mM PMSF, 2.5 mM EDTA, 0.5% Triton X-100, 0.5% NP-40, 5 μg/ml of aprotinin, pepstatin A, and leupeptin). The lysates were centrifuged at 15,000 rpm for 15 min at 4°C. Protein concentration was determined using 2D Quantification Kit (Amersham Biosciences). The protein samples (about 20 μg) were separated using SDS–PAGE. After SDS–PAGE electrophoresis, proteins were transferred to PVDF membranes. The membranes were blocked overnight at 4°C with 5% non-fat dry milk in TBS-T buffer (20 mM Tris, pH7.6, 100 mM $NaCl_2$, 0.5% Tween-20), followed by 3 h of incubation with the primary antibody (1:1,500–1:2,000 dilution) in TBS-T buffer containing 5% non-fat dry milk at room temperature. After washing three times with TBS-T buffer, the membranes were incubated with a horseradish peroxidase-conjugated goat anti-mouse IgG, goat anti-rabbit IgG or rabbit anti-goat IgG as a secondary antibody (1:3,000 dilution) for 1 h at room temperature. The membranes were then washed three times in TBS-T buffer and the reactions were visualized with ECL detection system. All of the Western blotting analyses were repeated at least three times.

IMMUNOHISTOCHEMISTRY AND TISSUE MICROARRAY

Tissue microarrays were obtained from U.S. Biomax, Inc. (Rockvile, MD). For the detection of human KRT8, PPA1, IDH2, and S100A11, we used tissue arrays containing cores from 155 serous adenocarcinomas, 33 mucinous adenocarcinomas, four adenocarcinomas, and 16 normal ovarian tissues in total (OV20810).

Immunohistochemistry (IHC) of tissue arrays was performed as described previously. Briefly, sections were warmed in a 60°C oven, dewaxed in three changes of xylene, and passaged through graded ethanol (100%, 95%, and 70%) before a final wash in double distilled H_2O. After quenching of endogenous peroxidase activity with 3% H_2O_2 for 10 min and blocking with BSA for 30 min, sections were incubated at 4°C overnight with antibodies against KRT8, PPA1, IDH2, and S100A11 at 1:200, 1:150, 1:200, and 1:250 dilution, respectively. Detection was achieved with the Envision/horseradish peroxidase system (Dako-Cytomation, Glostrup, Denmark). All slides were counterstained with Gill's hematoxylin for 1 min, dehydrated, and mounted for light microscopic evaluation. Protein expression was assessed using a semi-quantitative scoring consisting of an assessment of both staining intensity (scale 0–3) and the percentage of positive cells (0–100%), which, when multiplied, generate a Score ranging from 0 to 300. Interpretation of hematoxylin and eosin sections and analysis/scoring of TMA data were all done by the same certified pathologist to maintain consistency. Statistical analysis was done using SPSS v10.0 for Windows (SPSS Inc., Chicago, IL). The *t*-test was performed at 95% confidence.

S100A11 siRNA TRANSFECTION, WOUND HEALING ASSAY, AND INVASION ASSAY

For functional studies, two siRNA duplexes against human S100A11 (HSS109441 and HSS109443) and control siRNA were obtained from Invitrogen (Carlsbad, CA). ES-2 and SKOV-3 cells were first trypsinized in serum-free media and counted before transfection with 200 nM of luciferase control siRNA or S100A11-targeted siRNA using Lipofectamine 2000. Two days following transfection, the cells were seeded onto six-well plate and grown until a confluent monolayer. A wound was incised in the cell monolayer by using a sterile p200 pipette tip. The cells were washed once with growth medium to remove the cell debris and to smooth the edge of the scratch and then replaced with fresh growth medium. The cells were incubated at 37°C and their migration into the scratch area was monitored up to 16 h. Using a phase-contrast microscope, the images of the scratch at the same field were captured at 0 and 16 h after scratch. The relative width of the scratch was measured quantitatively using Adobe Photoshop 7.0. The extent of gap closure was determined as the rate of cell migration. For the invasion assay, about 1×10^5 transfected cells were added to the top chambers of 24-well transwell plate with polycarbonate membrane chambers coated with a uniform layer of dried basement membrane matrix solution (8 μm pore size; Cell Biolabs Inc., San Diego, CA) and medium containing 10% FBS were added to the bottom chambers. Incubation was done for 24 h. The top non-invasive cells were removed, and the bottom invaded cells were first dissociated from the membrane, then lysed and quantified at OD 560 nm. In all cases, effective knock down of gene expression was verified via Western blotting analysis described above. Experiments were performed at least in triplicates.

STATISTICAL ANALYSIS

The data were expressed as mean ± SD, and analyzed with the Student's *t*-test between two groups. It was considered statistically significant if *P*-value was <0.05.

RESULTS

DETECTION AND RELATIVE QUANTIFICATION OF PROTEINS IN NORMAL AND OVARIAN CANCER TISSUES

Total cellular proteins were extracted from the ovarian tissues as described in "Materials and Methods." Proteins were trypsin-

digested, labeled with iTRAQ reagents, and analyzed using tandem mass spectrometry to identify those protein abundance changes most likely attributable to the development and progression of ovarian cancer. For increasing the coverage of protein identification and/or the confidence of the data generated, samples were iTRAQ labeled in duplicate as follows (100 μg each per label): normal ovarian epithelial tissues, 113; ovarian cancer tissues, 114; normal ovarian epithelial tissues, 115; and ovarian cancer tissues, 116. The labeled peptide samples were then pooled and dried in a vacuum concentrator. To reduce extreme sample's complexity, a batch of 70 fractions was separated per iTRAQ experiment using strong cation exchange chromatography as described in the Materials and Methods Section. These fractions were then combined into 20 samples and analyzed by LC/MS/MS. A schematic flowchart of the iTRAQ method is shown in Figure 1A. The MS/MS spectrum of KRT8 (peptide sequence: ASLEAAIADAEQR) is illustrated in

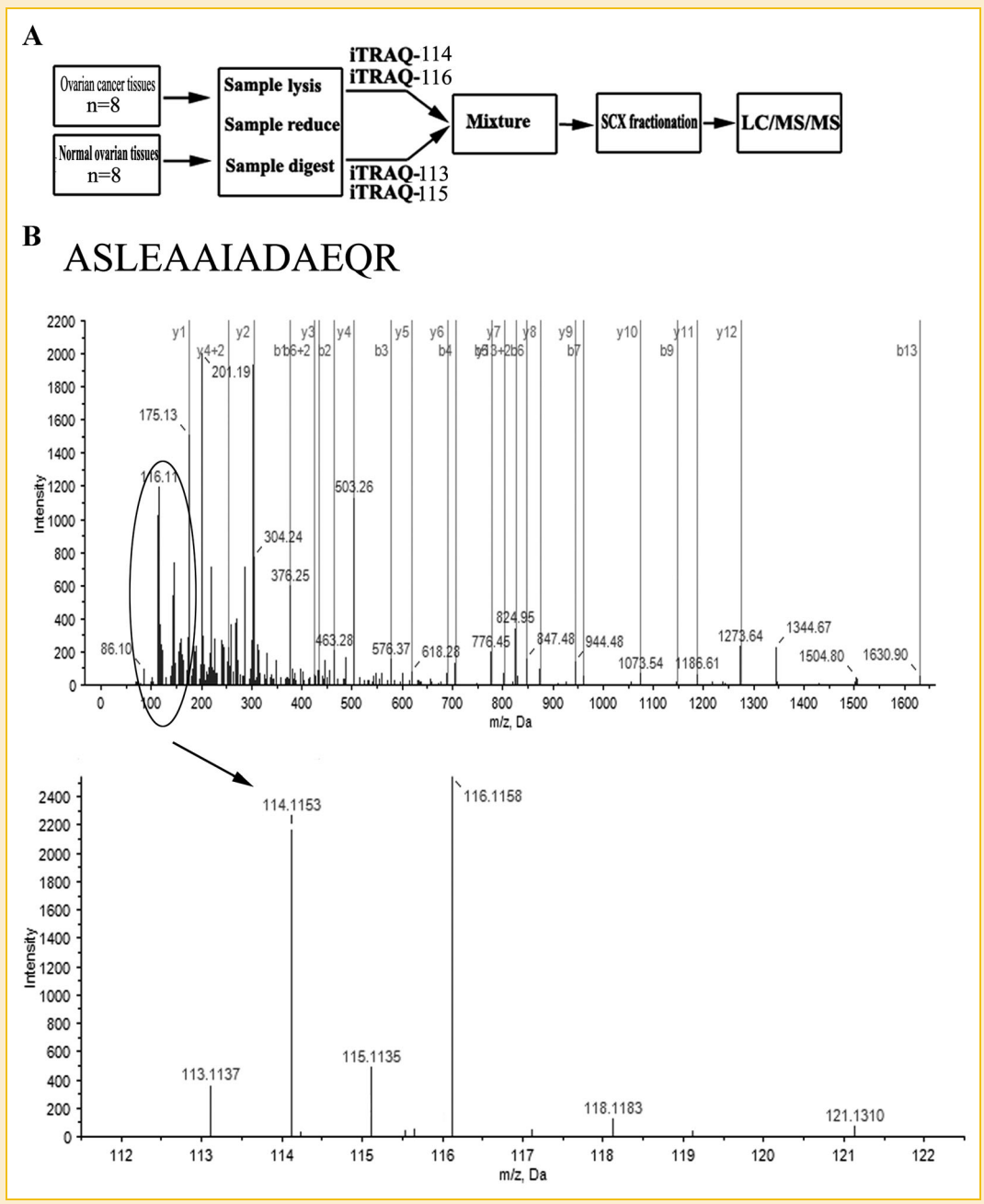

Fig. 1. The iTRAQ proteomics approach was used to identify potentially differentially expressed proteins in ovarian cancer tissues and normal ovarian tissues. A: Flow chart of iTRAQ proteomics approach. B: A representative MS/MS spectrum showing the peptides from KRT8 (peptide sequence: ASLEAAIADAEQR). Ovarian cancer tissues were labeled with iTRAQ 114 and 116 tags, and normal ovarian tissues were labeled with iTRAQ 113 and 115 tags. Thus, the ratio of 114:113 and 116:115 indicated the relative abundance of the KRT8 protein in ovarian cancer tissues compared with normal tissues.

Figure 1B. Normal ovarian epithelial tissues were labeled with iTRAQ 113 and 115 tags, and ovarian cancer tissues were labeled with iTRAQ 114 and 116 tags. Thus, the ratio of 114:113 and 116:115 would indicate the relative abundance of the KRT8 protein (Fig. 1B) in ovarian cancer tissues compared with normal tissues, respectively. When the same protein gave two similar relative quantitative ratios in both 114:113 and 116:115, the quantitation ratio is selected from the experiment with the best *P*-values. A total of 1,259 unique proteins were identified with 95% confidence by the ProteinPilot search algorithm against the IPI human protein database v3.49. Although relative quantification analysis by ProteinPilot 2.0 software come with statistical analysis and since most methods are prone to technical variation, we included an additional 1.3-fold change cutoff for all iTRAQ ratios to reduce false positives for the selection of potentially differentially expressed proteins. This filtering measure resulted in a final set of 205 potentially differentially expressed proteins between ovarian cancer tissues and normal ovarian tissues. Of those, 86 proteins were increased and 119 were decreased in ovarian cancer tissues compared with normal tissues. The iTRAQ data for all 205 proteins are found in Supplementary Table I, while only the top 60 up- and down-regulated proteins in both groups of cancer tissues compared with normal tissues are shown in Table I. These 205 proteins, which were potentially differentially expressed between the ovarian cancer tissues and normal ovarian tissues, could be classified into 22 functional categories using the PANTHER classification system (www.pantherdb.org; Fig. 2). The top five molecular functions categories were signaling molecule (12.8%), transfer/carrier protein (8.9%), nucleic acid-binding protein (8.9%), transferase (7.8%), and oxidoreductase (7.8%).

VALIDATION OF DIFFERENTIAL EXPRESSION PROTEINS

The potentially differential expression levels of the proteins identified by the iTRAQ approach were validated using Western blotting and real-time quantitative RT-PCR analyses. Figure 3A shows the relative mRNA expression levels of LAP3, IDH2, MX1, AGR2, THBS1, KRT8, KRT7, PSAT1, PPA1, EPPK1, S100A11, MFAP4, AOC3, and RBP1, as normalized to18S rRNA. The mRNA levels of LAP3, IDH2, MX1, AGR2, THBS1, KRT8, KRT7, PSAT1, PPA1, EPPK1, and S100A11, are up-regulated in the ovarian cancer tissues, whereas the mRNA levels of MFAP4, AOC3, and RBP1 are down-regulated, as compared to the normal tissues. This trend is similar to their protein expression levels obtained in iTRAQ approach. Figure 3B shows representative Western blot analysis results of KRT8, PPA1, IDH2, and S100A11 expressions in the ovarian cancer tissues. Compared with normal tissues, ovarian cancer tissues had an obvious up-regulation of KRT8, PPA1, IDH2, and S100A11.

VALIDATION OF KRT8, PPA1, IDH2, AND S100A11 OVEREXPRESSION BY IHC USING TISSUE MICROARRAYS

To assess the clinical relevance, we examined the expression of KRT8, PPA1, IDH2, and S100A11 in tissue microarrays containing 155 serous adenocarcinomas, 33 mucinous adenocarcinomas, four adenocarcinomas, and 16 normal ovarian tissues by IHC. The results showed that the highest levels of signal intensity were detected in specimens from malignant glands. As shown in Figure 4B, significant IHC score values of KRT8, PPA1, IDH2, and S100A11 are higher in ovarian cancer tissues than in normal tissues. For illustration of KRT8, 161/192 (83.9%) cases of ovarian cancers have IHC scores of >0 with no expression seen in normal ovarian tissues. Representative images of the IHC of KRT8, PPA1, IDH2, and S100A11 in normal and ovarian cancer tissues are shown in Figure 4A.

S100A11 PLAYS A ROLE IN OVARIAN CANCER CELL MIGRATION AND INVASION

Coupled to the existing knowledge on the function of the members in the S100 family and bioinformatics performed the collective data on the up-regulation of S100A11 expression proposed a testable hypothesis that S100A11 plays a role in ovarian cancer migration and invasion. To this end, human ovarian cancer cell lines ES-2 and SKOV-3 were first transfected with two S100A11-specific siRNA sequences and one control siRNA. Effective silencing of S100A11 expression was demonstrated by the S100A11-specific sequences but not the control siRNA both in the cell lysate of SKOV-3 (Fig. 5A) and ES-2 (data not shown). We then subject the control and S100A11-knock-down ovarian cancer cells to cell invasion and migration assays. As shown in Figure 5B, silencing of S100A11 by the two gene-specific siRNAs significantly inhibited the invasion in ovarian cell line ES-2 and SKOV-3 compared to control siRNA. Similarly, S100A11 knock-down led to a sharp reduction on the ability of the ES-2 and SKOV-3 to close the gap introduced by a scratch wound compared to control cells (Fig. 5C). Collectively, the data indicate that S100A11 plays a functional role in ovarian cancer cell invasion and more prominently in migration.

DISCUSSION

Ovarian cancer remains one of the leading causes of female death in the world, and therefore the discovery of the novel proteins related to carcinogenesis and progression of ovarian cancer for its diagnosis, prognosis, and treatment has the potential to improve the clinical strategy and outcome for this disease. In the present study, we used iTRAQ proteomic approach to identify proteins with potentially differential expression between ovarian cancer and normal ovarian epithelia tissues that might be associated with the development and progression of ovarian cancer. A total of 205 proteins were found to be potentially differentially expressed between ovarian cancer tissues and normal ovarian tissues. Fourteen of these, that is, LAP3, IDH2, MX1, AGR2, THBS1, KRT8, KRT7, PSAT1, PPA1, EPPK1, S100A11, MFAP4, AOC3, and RBP1, were confirmed using real-time RT-PCR analysis and/or Western blotting analysis. We further validated the expression of PPA1, IDH2, KRT8, and S100A11 in tissue microarrays containing 192 ovarian cancer tissues, and 16 normal ovarian tissues by IHC. In addition, interestingly enough, our approach led to the further characterization of S100A11 as highly correlated with the migration and invasion of ovarian cancer, which has never been reported before. It provides evidence that the iTRAQ reagents labeling method for the

TABLE I. Partial List of Proteins Identified to Be Expressed at Different Levels Between Normal Ovarian Tissues and Ovarian Cancer Tissues by iTraq Analysis

N	Accession	Gene sym	Name	Ovarian cancer:normal	*P*-value ovarian cancer:normal
Top 30 proteins down-regulated in ovarian cancer tissues					
1	IPI:IPI00022391.1	APCS	APCS serum amyloid P-component	0.10	2.44E−06
2	IPI:IPI00793751.2	MFAP4	Microfibril-associated glycoprotein 4	0.12	1.54E−03
3	IPI:IPI00657682.2	GSTA1	Glutathione *S*-transferase A1	0.12	7.70E−07
4	IPI:IPI00005563.1	TINAGL1	Isoform 1 of tubulointerstitial nephritis antigen-like	0.18	2.94E−02
5	IPI:IPI00550239.4	H1F0	Histone H1.0	0.26	4.61E−04
6	IPI:IPI00219038.9	H3F3B	Histone H3.3	0.26	3.98E−03
7	IPI:IPI00009771.6	LMNB2	Lamin-B2	0.26	1.62E−05
8	IPI:IPI00219718.3	RBP1	Retinol-binding protein 1, cellular isoform a	0.27	5.55E−06
9	IPI:IPI00004457.3	AOC3	Membrane primary amine oxidase	0.27	1.70E−05
10	IPI:IPI00844156.2	SERPINC1	SERPINC1 protein	0.28	4.17E−02
11	IPI:IPI00873982.2	MYH11	Myosin heavy chain 11 smooth muscle isoform	0.31	3.43E−06
12	IPI:IPI00394820.3	OLFML1	Olfactomedin-like protein 1	0.33	3.74E−04
13	IPI:IPI00783665.3	LAMA5	Laminin subunit alpha-5	0.34	2.26E−02
14	IPI:IPI00021924.1	H1FX	Histone H1x	0.34	1.16E−02
15	IPI:IPI00873589.1	MAOB	Monoamine oxidase B	0.35	7.35E−03
16	IPI:IPI00025465.2	OGN	Highly similar to mimecan	0.35	9.82E−16
17	IPI:IPI00009896.1	EPHX1	Epoxide hydrolase 1	0.36	1.37E−06
18	IPI:IPI00657860.1	BST1	Putative uncharacterized protein BST1	0.37	2.82E−02
19	IPI:IPI00024621.3	OLFML3	Isoform 1 of olfactomedin-like protein 3	0.37	2.39E−05
20	IPI:IPI00176903.2	PTRF	Isoform 1 of polymerase I and transcript release factor	0.39	2.78E−03
21	IPI:IPI00640817.1	AK1	Adenylate kinase 1	0.40	4.20E−03
22	IPI:IPI00644827.1	MFAP2	Microfibrillar-associated protein 2 isoform b precursor	0.41	4.83E−02
23	IPI:IPI00413451.1	SERPINB6	Putative uncharacterized protein DKFZp686I04222	0.42	5.61E−03
24	IPI:IPI00056334.5	PRKCDBP	Protein kinase C delta-binding protein	0.44	2.28E−02
25	IPI:IPI00012119.1	DCN	Isoform A of decorin	0.44	1.93E−21
26	IPI:IPI00011302.1	CD59	CD59 glycoprotein	0.44	3.90E−02
27	IPI:IPI00217950.5	HMGN2	Non-histone chromosomal protein HMG-17	0.44	7.40E−03
28	IPI:IPI00100980.9	EHD2	EH domain-containing protein 2	0.45	1.42E−02
29	IPI:IPI00181126.3	LOC649445	Similar to high mobility group nucleosomal binding domain 2 isoform 1	0.45	4.37E−02
30	IPI:IPI00156689.3	VAT1	Synaptic vesicle membrane protein VAT-1 homolog	0.46	2.52E−02
Top 30 proteins up-regulated in ovarian cancer tissues					
1	IPI:IPI00479722.2	PSME1	Proteasome activator complex subunit 1	1.89	1.89E−02
2	IPI:IPI00643196.1	PFKP	Phosphofructokinase, platelet	1.90	2.28E−02
3	IPI:IPI00884176.1	F13A1	Coagulation factor XIII A1 subunit precursor	1.91	2.53E−05
4	IPI:IPI00292150.4	LTBP2	Latent-transforming growth factor beta-binding protein 2	2.00	3.38E−02
5	IPI:IPI00795292.1	NME2	NME1-NME2 protein	2.01	8.37E−05
6	IPI:IPI00852987.1	TYMP	Highly similar to Homo sapiens endothelial cell growth factor 1 (platelet-derived) (ECGF1), mRNA	2.03	2.40E−02
7	IPI:IPI00177728.3	CNDP2	Cytosolic non-specific dipeptidase	2.05	5.27E−03
8	IPI:IPI00007797.3	FABP5	Fatty acid-binding protein, epidermal	2.05	7.55E−03
9	IPI:IPI00845263.1	FN1	Fibronectin 1 isoform 2 preproprotein	2.07	2.78E−13
10	IPI:IPI00449049.5	PARP1	Poly [ADP-ribose] polymerase 1	2.07	1.49E−02
11	IPI:IPI00555577.1	THY1	Thy-1 cell surface antigen variant (Fragment)	2.08	2.46E−03
12	IPI:IPI00010951.2	EPPK1	Epiplakin 1	2.11	4.92E−02
13	IPI:IPI00013895.1	S100A11	Protein S100-A11	2.12	1.12E−04
14	IPI:IPI00893729.1	FTL	Ferritin light polypeptide variant (fragment)	2.13	2.74E−03
15	IPI:IPI00015018.1	PPA1	Inorganic pyrophosphatase	2.20	2.39E−02
16	IPI:IPI00479186.6	PKM2	Highly similar to pyruvate kinase isozyme M1	2.38	1.52E−04
17	IPI:IPI00021885.1	FGA	Isoform 1 of fibrinogen alpha chain	2.63	4.83E−17
18	IPI:IPI00908873.1	NOLC1	Isoform 3 of nucleolar phosphoprotein p130	2.68	4.51E−03
19	IPI:IPI00219713.1	FGG	Isoform gamma-A of fibrinogen gamma chain	2.84	4.08E−17
20	IPI:IPI00419237.3	LAP3	Isoform 1 of cytosol aminopeptidase	2.96	1.18E−06
21	IPI:IPI00298497.3	FGB	Fibrinogen beta chain	3.13	1.12E−19
22	IPI:IPI00011107.2	IDH2	Isocitrate dehydrogenase [NADP], mitochondrial	3.33	5.82E−03
23	IPI:IPI00167949.6	MX1	Interferon-induced GTP-binding protein Mx1	3.78	2.31E−02
24	IPI:IPI00893881.1	AGR2	Anterior gradient 2 homolog (fragment)	3.88	2.18E−03
25	IPI:IPI00479145.2	KRT19	Keratin, type I cytoskeletal 19	4.17	2.22E−07
26	IPI:IPI00296099.6	THBS1	Thrombospondin-1	4.28	7.97E−05
27	IPI:IPI00554648.3	KRT8	Keratin, type II cytoskeletal 8	6.13	2.98E−16
28	IPI:IPI00554788.5	KRT18	Keratin, type I cytoskeletal 18	6.52	2.53E−08
29	IPI:IPI00847342.1	KRT7	Keratin 7	8.30	3.72E−11
30	IPI:IPI00001734.3	PSAT1	Highly similar to phosphoserine aminotransferase	10.77	3.57E−02

Only the top 30 up- and down-regulated proteins in ovarian cancer tissues are shown. Statistical calculation for iTRAQ-based detection and relative quantification were calculated using the Paragon Algorithm in the ProteinPilot™ software.

large-scale protein quantification was powerful and reliable. Based on the PANTHER classification system, all of the 205 proteins could be classified into 22 functional categories. We discuss some of the key proteins discovered in this work in the following text.

In our iTRAQ works, S100A11 was highly expressed in the ovarian cancer tissues, and expression level changes of S100A11 were confirmed by Western blotting analysis and real-time quantitative RT-PCR analysis. S100 proteins belong to the EF-

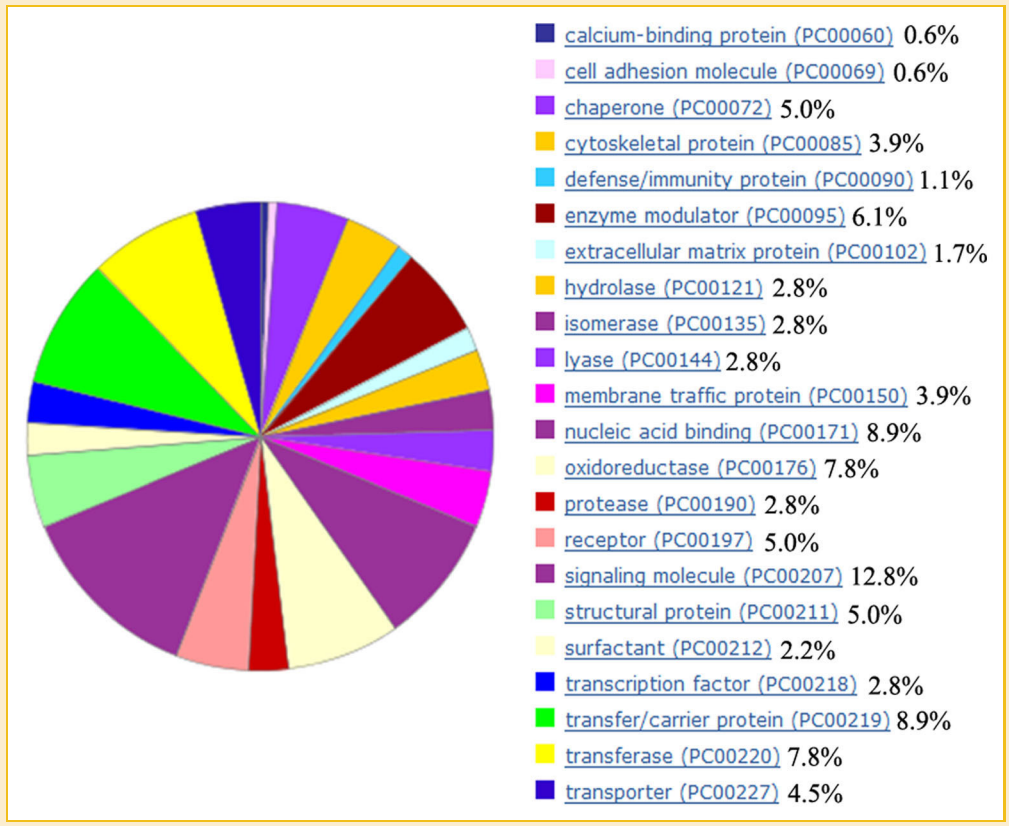

Fig. 2. Pie chart showing the various functional categories as a percentage of the 205 potentially differentially expressed proteins based on the PANTHER classification system.

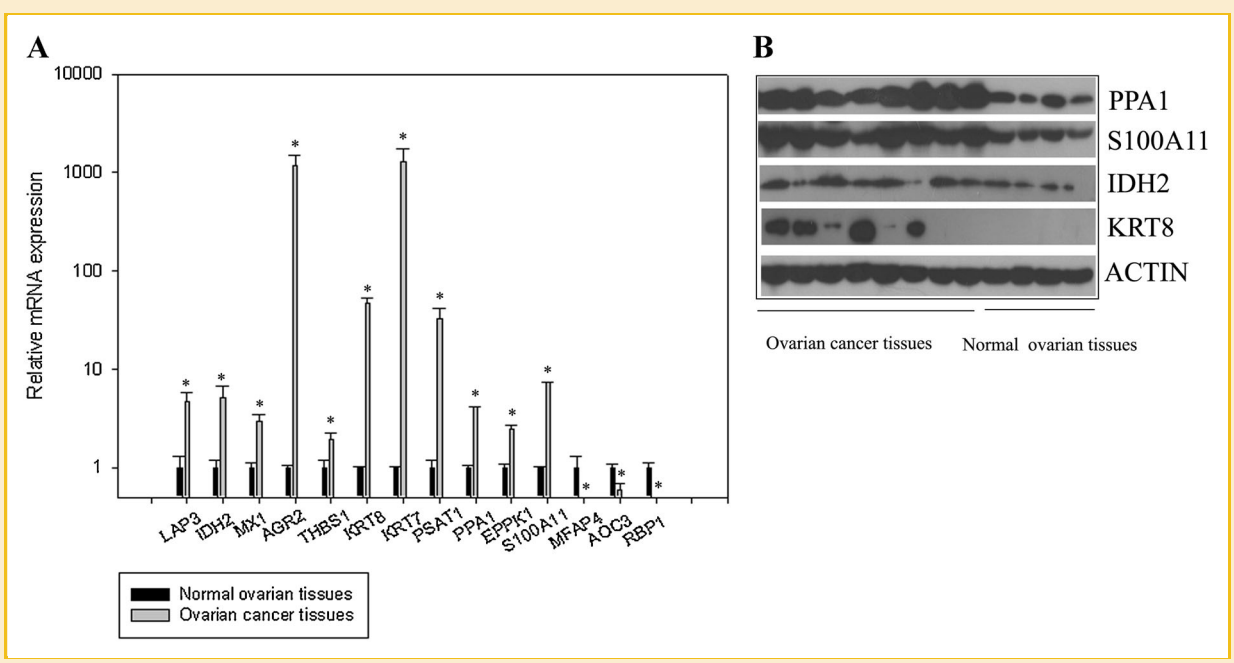

Fig. 3. Evaluation of the potentially differentially expressed proteins in ovarian cancer tissues and normal ovarian tissues. A: Real-time RT-PCR detected the relative mRNA expression levels of LAP3, IDH2, MX1, AGR2, THBS1, KRT8, KRT7, PSAT1, PPA1, EPPK1, S100A11, MFAP4, AOC3, and RBP1. 18S rRNA was used as the normalization standard. Compared with normal tissues, ovarian cancer tissues had an obvious up-regulation of LAP3, IDH2, MX1, AGR2, THBS1, KRT8, KRT7, PSAT1, PPA1, EPPK1, and S100A11, and down-regulation of MFAP4, AOC3, and RBP1, which were identical with the protein level changes in iTRAQ analysis. Bars indicate SD. $^{*}P \leq 0.05$ differ from control by *t*-test. B: A representative Western blotting analysis result of KRT8, IDH2, PPA1, and S100A11 expression in ovarian cancer tissues and normal ovarian tissues. Compared with normal tissues, ovarian cancer had an obvious up-regulation of KRT8, IDH2, PPA1, and S100A11.

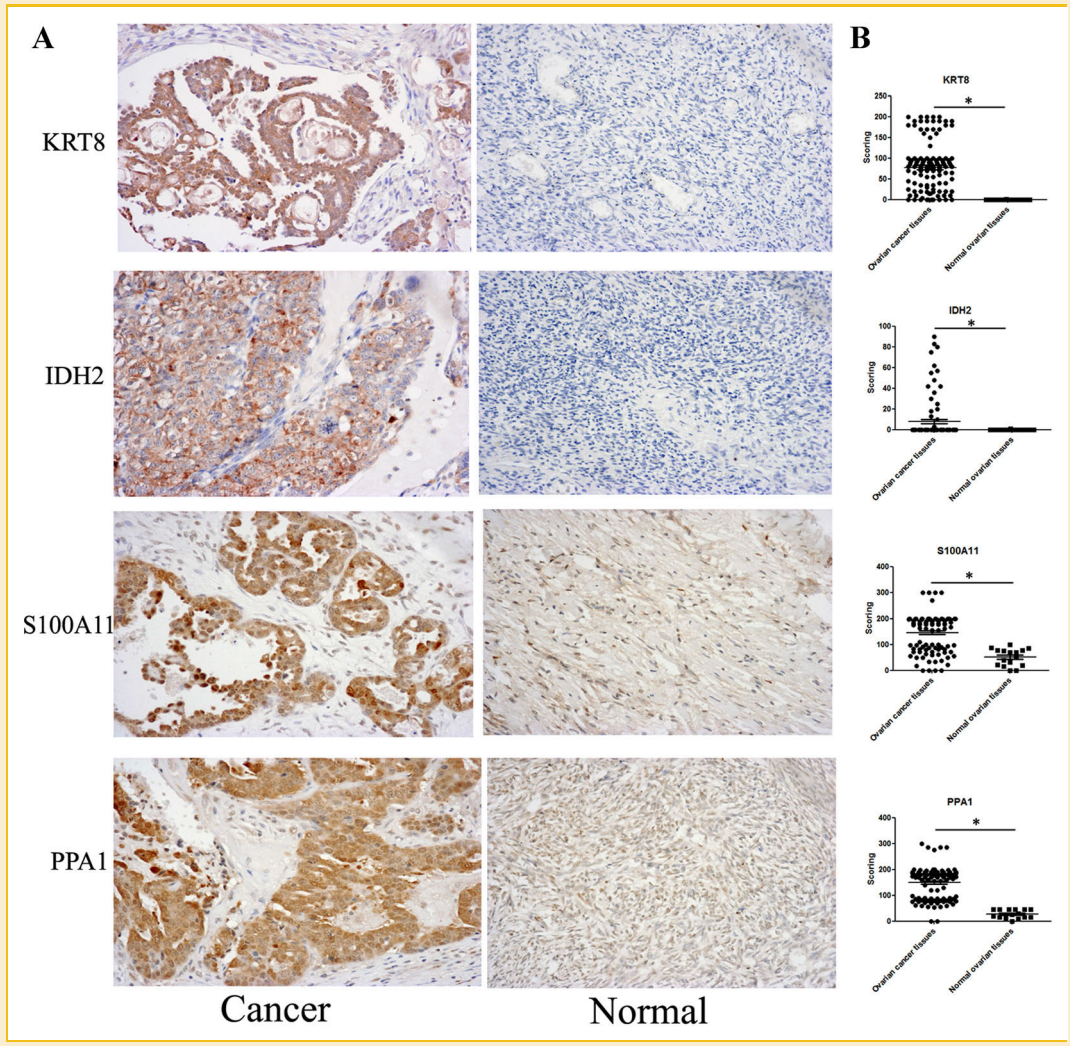

Fig. 4. Validation of KRT8, PPA1, IDH2, and S100A11 overexpression using tissue microarrays. A: Representative images of the immunohistochemistry of KRT8, IDH2, PPA1, and S100A11 expression in ovarian cancer tissues and normal ovarian tissues. B: Significant IHC score values of KRT8, PPA1, IDH2, and S100A11 are higher in ovarian cancer tissues than in normal tissues.

hand calcium-binding protein family, regulating a variety of intracellular and extracellular processes, including cell proliferation, differentiation, and intracellular signaling [Donato, 2001]. S100A11 is expressed in various tissues including placenta, heart, lung, and kidney [Inada et al., 1999]. It was also reported that S100A11 is overexpressed in gastric, pancreatic, colorectal, and prostate cancers, while significantly down-regulated in bladder cancer [Oue et al., 2004; Rehman et al., 2004; Memon et al., 2005; Melle et al., 2006; Ohuchida et al., 2006b]. Ohuchida et al. [2006ab] found that expression of S100A11 is increased in the early stage of pancreatic carcinogenesis and decreased during subsequent progression to cancer. In bladder cancer, loss of S100A11 is associated with poor survival in patients, and S100A11 expression is suppressed early during bladder cancer development [Rehman et al., 2004]. Despite these findings, the normal and pathogenic functions of S100A11 have remained largely unknown. Sakaguchi and Huh [2011] demonstrated that S100A11 plays a dual role in growth regulation of epithelial cells. On one hand, S100A11 is a key mediator of high Ca^{2+} and TGF-β induced growth inhibition of epithelial cells, and blocking the S100A11-mediated pathway abrogated the growth suppression of cells. On the other hand, secreted S100A11 can act on the cells to promote cell growth via induction of EGF [Sakaguchi et al., 2003, 2004, 2008]. Due to the role of S100A11 in ovarian cancer has not been investigated, thus we evaluated the expression of S100A11 in ovarian cancer tissues using microarrays. Our results demonstrated that the S100A11 expression was significantly higher in clinical ovarian cancer samples than in normal ovarian samples, suggesting that it is a promising candidate for future biomarker development. Furthermore, siRNA-mediated down-regulation of S100A11 expression significantly decreased in vitro both invasive ability and migration potential of ES-2 and SKOV-3 cell lines, which further indicated that S100A11 could serve as a potential target for anti-ovarian cancer therapy.

Ubiquitously expressed cytoskeletal proteins, such as KRT8, KRT18, and KRT7 were found to be remarkably different in ovarian

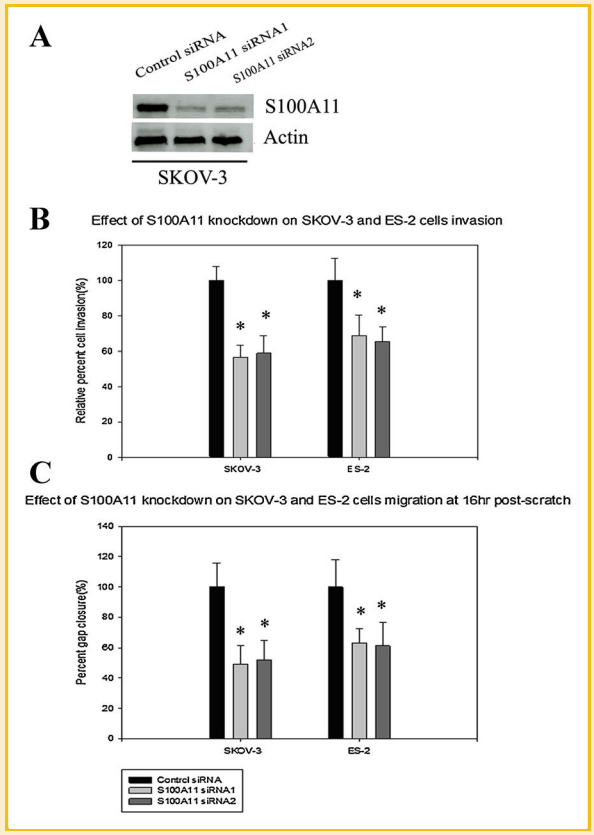

Fig. 5. Functional studies of S100A11 in ovarian cancer cell migration and invasion. A: Western blotting analysis showed that transfection of cells with two S100A11-specific siRNAs significantly reduced S100A11 protein levels both in the cell lysate of SKOV-3 and ES-2 (data not shown). B: Silencing of S100A11 by the two gene-specific siRNAs significantly inhibited the invasion properties of ovarian cell lines ES-2 and SKOV-3 compared to control siRNA. C: S100A11 knock-down led to a sharp reduction in the ability of the ES-2 and SKOV-3 cells to close the gap introduced by a scratch wound, compared to control cells.

cancer tissues, compared to normal tissues. Therefore, we further examined the expression of KRT8 in tissue microarrays, and demonstrated that KRT8 expression was observed in about 83.9% cases of ovarian cancers and not seen in normal ovarian tissues. In recent years, KRT8 has been correlated with increased invasiveness in lung cancer, breast cancer and esophageal cancer, and involved in the development of multidrug resistance of breast cancer [Tojo et al., 2003; Liu et al., 2008; Bartkowiak et al., 2009; Makino et al., 2009]. Several reports have demonstrated that KRT8 is a potential plasminogen receptor and able to promote plasminogen activation through tissue-type plasminogen activator on the cancer cell surface [Hembrough et al., 1995; Hembrough et al., 1996; Gonias et al., 2001]. Numerous studies have demonstrated that plasminogen activators promote tumor cell invasion, suggesting that KRT8 may play an important role in progression of ovarian cancer.

Up-regulation of the anterior gradient 2 protein (AGR2) was also observed in our study. AGR2 is a secreted protein that has been reported in a number of cancers including breast, prostate, and lung cancers, although its functional role in cancer is believed to be limited [Fritzsche et al., 2006, 2007; Kovalev et al., 2006]. Pohler et al. [2004] reported that cells overexpressing AGR2 attenuate p53 phosphorylation and silence p53 transactivation function in ultraviolet-damaged cells, suggesting that AGR2 functions as a survival factor through inhibition of p53. Furthermore, AGR2 modulated breast cancer drivers, including cyclin D1, c-*Myc*, and ER, as well as more general oncogenic signaling nodes, such as p-Src and survivin [Vanderlaag et al., 2010]. In the present study, our results showed that AGR2 was overexpressed in ovarian cancer tissues, and the mRNA level of AGR2 gene was almost 1,300-fold higher in ovarian cancer tissues than in normal ovarian tissues. These data strongly indicated that ARG2 plays an important functional role in ovarian cancer.

Decorin is a small proteoglycan, which regulated a variety of functions in the extracellular matrix including collagen fibrillogenesis, collagen degradation, and extracellular signaling [Iozzo et al., 1999; Reed and Iozzo, 2002; Bhide et al., 2005; Seidler et al., 2006; Goldoni et al., 2008]. Importantly, decorin has been shown to exert powerful growth-inhibitory properties through up-regulation of the cell cycle inhibitor p21 and p27, down-regulation of epidermal growth factor receptor (EGFR), and blockade of transforming growth factor-β1 pathway [Yamaguchi et al., 1990; De Luca et al., 1996; Iozzo et al., 1999; Xaus et al., 2001]. Nash et al. [2002] examined the inhibitory effects of decorin on the growth of ovarian tumor cells, and confirmed that decorin-induced inhibition of ovarian tumor cells appeared to be associated with the increased expression of the cyclin-dependent kinase inhibitor p21. Therefore, it is very likely that decorin down-regulation in ovarian cancer tissues correlated with the development of ovarian cancer.

Finally, our study identified several proteins, including PSAT1, PPA1, and IDH2, which had not been associated with ovarian cancer previously, but had been implicated in tumor progression. Recent retrospective studies have found a major favorable prognostic effect of the presence of IDH1 and IDH2 mutations on survival of grades II and III glial tumors [van den Bent et al., 2006]. It is possible that IDH2 mutations may exist in the ovarian cancer specimens tested in our study. The correlation between each of the potentially differentially expressed proteins and ovarian cancer will be a focus of our future study.

Ovarian cancer remains the leading cause of death attributable to gynecological cancers in the world. Therefore, there is an urgent need for improved diagnosis and prognosis of ovarian cancer. In this study, we focused our attention on those proteins that changed in expression levels in ovarian cancer tissues. As a result, 205 potentially differentially expressed proteins possibly associated with development and progression of ovarian cancer were identified, and the correlation of S100A11, KRT8, PPA1, and IDH2 with ovarian cancer was verified. These data are valuable for further study of the mechanism of carcinogenesis in human ovarian cancer, and greatly expanded the number of our candidate biomarkers for ovarian cancer.

ACKNOWLEDGMENTS

This work was supported by program for Changjiang Scholars and Innovative Research Team in University (no. IRT0872), National

Natural Science Foundation of China (no. 30801348, and 30900507), National Science and Technology Major Project of China (no. 2008ZX10002-006), and China Postdoctoral Science Foundation Founded Project (no. 20070410210).

REFERENCES

Banerjee S, Gore M. 2009. The future of targeted therapies in ovarian cancer. Oncologist 14:706–716.

Bartkowiak K, Wieczorek M, Buck F, Harder S, Moldenhauer J, Effenberger KE, Pantel K, Peter-Katalinic J, Brandt BH. 2009. Two-dimensional differential gel electrophoresis of a cell line derived from a breast cancer micrometastasis revealed a stem/progenitor cell protein profile. J Proteome Res 8:2004–2014.

Bhide VM, Laschinger CA, Arora PD, Lee W, Hakkinen L, Larjava H, Sodek J, McCulloch CA. 2005. Collagen phagocytosis by fibroblasts is regulated by decorin. J Biol Chem 280:23103–23113.

Cortesi L, Rossi E, Della Casa L, Barchetti A, Nicoli A, Piana S, Abrate M, La Sala GB, Federico M, Iannone A. 2011. Protein expression patterns associated with advanced stage ovarian cancer. Electrophoresis 32:1992–2003.

De Luca A, Santra M, Baldi A, Giordano A, Iozzo RV. 1996. Decorin-induced growth suppression is associated with up-regulation of p21, an inhibitor of cyclin-dependent kinases. J Biol Chem 271:18961–18965.

Donato R. 2001. S100: A multigenic family of calcium-modulated proteins of the EF-hand type with intracellular and extracellular functional roles. Int J Biochem Cell Biol 33:637–668.

Fritzsche FR, Dahl E, Pahl S, Burkhardt M, Luo J, Mayordomo E, Gansukh T, Dankof A, Knuechel R, Denkert C, Winzer KJ, Dietel M, Kristiansen G. 2006. Prognostic relevance of AGR2 expression in breast cancer. Clin Cancer Res 12:1728–1734.

Fritzsche FR, Dahl E, Dankof A, Burkhardt M, Pahl S, Petersen I, Dietel M, Kristiansen G. 2007. Expression of AGR2 in non small cell lung cancer. Histol Histopathol 22:703–708.

Goldoni S, Seidler DG, Heath J, Fassan M, Baffa R, Thakur ML, Owens RT, McQuillan DJ, Iozzo RV. 2008. An antimetastatic role for decorin in breast cancer. Am J Pathol 173:844–855.

Gonias SL, Hembrough TA, Sankovic M. 2001. Cytokeratin 8 functions as a major plasminogen receptor in select epithelial and carcinoma cells. Front Biosci 6:D1403–D1411.

Gygi SP, Rist B, Gerber SA, Turecek F, Gelb MH, Aebersold R. 1999. Quantitative analysis of complex protein mixtures using isotope-coded affinity tags. Nat Biotechnol 17:994–999.

Hembrough TA, Vasudevan J, Allietta MM, Glass WF II, Gonias SL. 1995. A cytokeratin 8-like protein with plasminogen-binding activity is present on the external surfaces of hepatocytes, HepG2 cells and breast carcinoma cell lines. J Cell Sci 108(Pt 3):1071–1082.

Hembrough TA, Kralovich KR, Li L, Gonias SL. 1996. Cytokeratin 8 released by breast carcinoma cells in vitro binds plasminogen and tissue-type plasminogen activator and promotes plasminogen activation. Biochem J 317(Pt 3):763–769.

Inada H, Naka M, Tanaka T, Davey GE, Heizmann CW. 1999. Human S100A11 exhibits differential steady-state RNA levels in various tissues and a distinct subcellular localization. Biochem Biophys Res Commun 263:135–138.

Iozzo RV, Moscatello DK, McQuillan DJ, Eichstetter I. 1999. Decorin is a biological ligand for the epidermal growth factor receptor. J Biol Chem 274:4489–4492.

Kim JM, Sohn HY, Yoon SY, Oh JH, Yang JO, Kim JH, Song KS, Rho SM, Yoo HS, Kim YS, Kim JG, Kim NS. 2005. Identification of gastric cancer-related genes using a cDNA microarray containing novel expressed sequence tags expressed in gastric cancer cells. Clin Cancer Res 11:473–482.

Kovalev LI, Shishkin SS, Khasigov PZ, Dzeranov NK, Kazachenko AV, Kovaleva MA, Toropygin I, Eremina LS, Grachev SV. 2006. New approaches to molecular diagnosis of prostatic cancer. Urologiia 5:16–19.

Liu F, Chen Z, Wang J, Shao X, Cui Z, Yang C, Zhu Z, Xiong D. 2008. Overexpression of cell surface cytokeratin 8 in multidrug-resistant MCF-7/MX cells enhances cell adhesion to the extracellular matrix. Neoplasia 10:1275–1284.

Livak KJ, Schmittgen TD. 2001. Analysis of relative gene expression data using real-time quantitative PCR and the 2(-Delta Delta C(T)) method. Methods 25:402–408.

Makino T, Yamasaki M, Takeno A, Shirakawa M, Miyata H, Takiguchi S, Nakajima K, Fujiwara Y, Nishida T, Matsuura N, Mori M, Doki Y. 2009. Cytokeratins 18 and 8 are poor prognostic markers in patients with squamous cell carcinoma of the oesophagus. Br J Cancer 101:1298–1306.

Melle C, Ernst G, Schimmel B, Bleul A, Mothes H, Kaufmann R, Settmacher U, Von Eggeling F. 2006. Different expression of calgizzarin (S100A11) in normal colonic epithelium, adenoma and colorectal carcinoma. Int J Oncol 28:195–200.

Memon AA, Sorensen BS, Meldgaard P, Fokdal L, Thykjaer T, Nexo E. 2005. Down-regulation of S100C is associated with bladder cancer progression and poor survival. Clin Cancer Res 11:606–611.

Mirgorodskaya OA, Kozmin YP, Titov MI, Korner R, Sonksen CP, Roepstorff P. 2000. Quantitation of peptides and proteins by matrix-assisted laser desorption/ionization mass spectrometry using (18)O-labeled internal standards. Rapid Commun Mass Spectrom 14:1226–1232.

Mok SC, Chao J, Skates S, Wong K, Yiu GK, Muto MG, Berkowitz RS, Cramer DW. 2001. Prostasin, a potential serum marker for ovarian cancer: Identification through microarray technology. J Natl Cancer Inst 93:1458–1464.

Nash MA, Deavers MT, Freedman RS. 2002. The expression of decorin in human ovarian tumors. Clin Cancer Res 8:1754–1760.

Ohuchida K, Mizumoto K, Egami T, Yamaguchi H, Fujii K, Konomi H, Nagai E, Yamaguchi K, Tsuneyoshi M, Tanaka M. 2006a. S100P is an early developmental marker of pancreatic carcinogenesis. Clin Cancer Res 12:5411–5416.

Ohuchida K, Mizumoto K, Ohhashi S, Yamaguchi H, Konomi H, Nagai E, Yamaguchi K, Tsuneyoshi M, Tanaka M. 2006b. S100A11, a putative tumor suppressor gene, is overexpressed in pancreatic carcinogenesis. Clin Cancer Res 12:5417–5422.

Oue N, Hamai Y, Mitani Y, Matsumura S, Oshimo Y, Aung PP, Kuraoka K, Nakayama H, Yasui W. 2004. Gene expression profile of gastric carcinoma: Identification of genes and tags potentially involved in invasion, metastasis, and carcinogenesis by serial analysis of gene expression. Cancer Res 64:2397–2405.

Petricoin EF, Ardekani AM, Hitt BA, Levine PJ, Fusaro VA, Steinberg SM, Mills GB, Simone C, Fishman DA, Kohn EC, Liotta LA. 2002. Use of proteomic patterns in serum to identify ovarian cancer. Lancet 359:572–577.

Pohler E, Craig AL, Cotton J, Lawrie L, Dillon JF, Ross P, Kernohan N, Hupp TR. 2004. The Barrett's antigen anterior gradient-2 silences the p53 transcriptional response to DNA damage. Mol Cell Proteomics 3:534–547.

Reed CC, Iozzo RV. 2002. The role of decorin in collagen fibrillogenesis and skin homeostasis. Glycoconj J 19:249–255.

Rehman I, Azzouzi AR, Cross SS, Deloulme JC, Catto JW, Wylde N, Larre S, Champigneuille J, Hamdy FC. 2004. Dysregulated expression of S100A11 (calgizzarin) in prostate cancer and precursor lesions. Hum Pathol 35:1385–1391.

Ross PL, Huang YN, Marchese JN, Williamson B, Parker K, Hattan S, Khainovski N, Pillai S, Dey S, Daniels S, Purkayastha S, Juhasz P, Martin S, Bartlet-Jones M, He F, Jacobson A, Pappin DJ. 2004. Multiplexed protein quantitation in *Saccharomyces cerevisiae* using amine-reactive isobaric tagging reagents. Mol Cell Proteomics MCP 3:1154–1169.

Sakaguchi M, Huh NH. 2011. S100A11, a dual growth regulator of epidermal keratinocytes. Amino Acids 41:797–807.

Sakaguchi M, Miyazaki M, Takaishi M, Sakaguchi Y, Makino E, Kataoka N, Yamada H, Namba M, Huh NH. 2003. S100C/A11 is a key mediator of Ca(2+)-induced growth inhibition of human epidermal keratinocytes. J Cell Biol 163:825–835.

Sakaguchi M, Miyazaki M, Sonegawa H, Kashiwagi M, Ohba M, Kuroki T, Namba M, Huh NH. 2004. PKCalpha mediates TGFbeta-induced growth inhibition of human keratinocytes via phosphorylation of S100C/A11. J Cell Biol 164:979–984.

Sakaguchi M, Sonegawa H, Murata H, Kitazoe M, Futami J, Kataoka K, Yamada H, Huh NH. 2008. S100A11, an dual mediator for growth regulation of human keratinocytes. Mol Biol Cell 19:78–85.

Seidler DG, Goldoni S, Agnew C, Cardi C, Thakur ML, Owens RT, McQuillan DJ, Iozzo RV. 2006. Decorin protein core inhibits in vivo cancer growth and metabolism by hindering epidermal growth factor receptor function and triggering apoptosis via caspase-3 activation. J Biol Chem 281:26408–26418.

Tojo Y, Bandoh S, Fujita J, Kubo A, Ishii T, Fukunaga Y, Ueda Y, Yang Y, Wu F, Huang CL, Yokomise H, Ishida T. 2003. Aberrant messenger RNA splicing of the cytokeratin 8 in lung cancer. Lung Cancer 42:153–161.

van den Bent MJ, Carpentier AF, Brandes AA, Sanson M, Taphoorn MJ, Bernsen HJ, Frenay M, Tijssen CC, Grisold W, Sipos L, Haaxma-Reiche H, Kros JM, van Kouwenhoven MC, Vecht CJ, Allgeier A, Lacombe D, Gorlia T. 2006. Adjuvant procarbazine, lomustine, and vincristine improves progression-free survival but not overall survival in newly diagnosed anaplastic oligodendrogliomas and oligoastrocytomas: A randomized European Organisation for Research and Treatment of Cancer Phase III Trial. J Clin Oncol 24:2715–2722.

Vanderlaag KE, Hudak S, Bald L, Fayadat-Dilman L, Sathe M, Grein J, Janatpour MJ. 2010. Anterior gradient-2 plays a critical role in breast cancer cell growth and survival by modulating cyclin D1, estrogen receptor-alpha and survivin. Breast Cancer Res 12:R32.

Wulfkuhle JD, Sgroi DC, Krutzsch H, McLean K, McGarvey K, Knowlton M, Chen S, Shu H, Sahin A, Kurek R, Wallwiener D, Merino MJ, Petricoin EF III, Zhao Y, Steeg PS. 2002. Proteomics of human breast ductal carcinoma in situ. Cancer Res 62:6740–6749.

Xaus J, Comalada M, Cardo M, Valledor AF, Celada A. 2001. Decorin inhibits macrophage colony-stimulating factor proliferation of macrophages and enhances cell survival through induction of p27(Kip1) and p21(Waf1). Blood 98:2124–2133.

Yamaguchi Y, Mann DM, Ruoslahti E. 1990. Negative regulation of transforming growth factor-beta by the proteoglycan decorin. Nature 346:281–284.

Yurkovetsky Z, Skates S, Lomakin A, Nolen B, Pulsipher T, Modugno F, Marks J, Godwin A, Gorelik E, Jacobs I, Menon U, Lu K, Badgwell D, Bast RC, Jr., Lokshin AE. 2010. Development of a multimarker assay for early detection of ovarian cancer. J Clin Oncol 28:2159–2166.